Age-associated dysregulation of microglial activation is coupled with enhanced BBB permeability and pathology in APP/PS1 mice

Aedín M. Minogue[†]*, Raasay S. Jones[†], Ronan J. Kelly, Claire L. McDonald, Thomas J. Connor and Marina A. Lynch.

Trinity College Institute of Neuroscience,

Lloyd Building,

Trinity College,

Dublin 2,

Ireland.

† These authors contributed equally to the work.

*Correspondance: Email: aminogu@tcd.ie; Tel: 353-1-896-8476; Fax: 353-1-896-3545.

Running title: altered microglial activation states in aged APP/PS1 mice

Abstract

Aging adversely affects inflammatory processes in the brain, which has important implications in the context of disease progression. It has been proposed that microglia become dysfunctional with age and may lose their neuroprotective properties leading to chronic neurodegeneration. Here, we sought to characterize inflammatory changes in a mouse model of AD and to delineate differences between normal aging and those associated with disease pathology. A proinflammatory profile, characterized by upregulation of markers of classical activation was evident in APP/PS1 mice, associated with increased interferon (IFN)γ concentration and dysregulation of mechanisms designed to limit the proinflammatory response. The data indicate that microglia are not less active with age but alter their phenotype; indeed changes observed in the deactivation state appear to relate to aging rather than disease pathology. We hypothesize that disruption of the BBB, in tandem with an enhanced chemokine profile, permits the infiltration of immune cells serving to reinforce classical activation of microglia through their enhanced responsiveness to IFNγ.

Key words: Alzheimer's disease, microglial activation states, interferon-γ, blood brain barrier permeability, infiltrating immune cells

Introduction

Alzheimer's disease (AD) is characterized by the presence of amyloid plaques and neurofibrillary tangles, found in close association with activated microglia and astrocytes, an observation that has led to extensive investigation into the role of inflammation in disease pathophysiology. A compromised immune system, associated with aging, may negatively impact on inflammatory processes and lead to impaired brain function and neuronal repair, which in turn enhance the progression of AD. The blood brain barrier (BBB) functions to protect the brain from potentially damaging peripheral immune cells (Zlokovic, 2002) and a number of neuroinflammatory conditions, including AD, are associated with BBB disruption (Avison *et al*., 2004) and transendothelial migration of peripheral leukocytes (Togo *et al*., 2002).

Similar to tissue macrophages, microglia respond to inflammatory stimuli in the CNS in a pre-programmed manner designed to defend the brain against the effects of insult but also to initiate repair and restore homeostasis (Czeh *et al*., 2011). These cells can be classified into three major subsets, and further intermediate ones, with discrete molecular phenotypes and effector functions depending on the activation pathways elicited. Classical activation, stimulated by the Th1 cytokine interferon (IFN)γ, is identified by upregulation of tumour necrosis factor (TNF)α and inducible nitric oxide synthase (iNOS) and is associated with inflammation, extracellular matrix destruction and, in some cases, apoptosis (Mosser and Edwards, 2008). In contrast, alternative activation and acquired deactivation are stimulated by the anti-inflammatory cytokines IL-4 and IL-10 respectively and are associated with cellular and tissue repair and return to homeostasis (Mosser, 2003). Since identification of the classical, alternative and acquired deactivation inflammatory states in the periphery (Martinez *et al*., 2009), and to some extent in the brain (Colton *et al*., 2006), it has become clear that the contribution of inflammation to neurodegenerative processes may be far more varied than originally postulated. While reports detailing the role of classical activation in AD are numerous, less work has been carried out investigating the changes in alternative activation and acquired deactivation. One recent study,

however, has suggested increases in markers of alternative activation such as mannose receptor (MRC1) and arginase-1 in the Tg2576 mouse model of AD (Colton *et al*., 2006). As such, a hybrid activation state incorporating characteristics of both classical and alternative activation has been hypothesized to play a role in AD.

The recognition that mutations in presenilin (PS) 1 and duplication of the amyloid precursor protein (APP) gene are the most commonly-recognized causes of familial AD (FAD) led to the development of a transgenic mouse model (APPswe/PS1dE9) that mimics some of the pathology associated with disease progression. Pathogenic mutations on PS, for example the Asn141 → Ile PS2 mutation (Mann *et al*., 1997), deletion of exon 10 of PS1 (Ishii *et al*., 1997, Mann *et al*., 1997) or FAD-linked mutations in PS1 and PS2 (Scheuner *et al*., 1996), have been coupled with increased $A\beta_{1\text{-}42}$ production and this also occurs in the brains of transgenic mice overexpressing mutated PS1 alone (Borchelt *et al*., 1996, Duff *et al*., 1996, Citron *et al*., 1997) or in combination with mutated β-APP (Borchelt *et al*., 1996, Holcomb *et al*., 1998). In this study, we used the APPswe/PS1dE9 (APP/PS1) mouse model to investigate the possible mechanisms that induce microglia to adopt different activation states in the hippocampus with age. The data indicate that an age-related accumulation of Aβ was accompanied by increased expression of markers of classical activation and decreased expression of those associated with acquired deactivation. We propose that infiltration of IFNγ-producing immune cells, likely as a consequence of increased BBB permeability, triggers microglia to adopt a classical proinflammatory phenotype with age in APP/PS1 mice.

Materials and Methods

Animals

Groups of 14 (*n*=7-8) and 24 month-old (*n*=4-8) APP/PS1 mice and wildtype littermate controls (male = 12, female = 15) were used in this study. Mice, initially purchased from The Jackson Laboratory (USA), were bred with C57BL/6 animals in a specific pathogen-free environment at the BioResources

Unit of Trinity College Dublin. All experimental work was performed under a licence granted by the Minister for Health and Children (Ireland) under the Cruelty to Animals Act 1876 and the European Community Directive 86/609/EEC. In a second experiment, a cohort of 18 month-old (*n*=7-8; male = 7, female = 8) wildtype and APP/PS1 mice were used to investigate the presence of infiltrating peripheral immune cells in the brains of these animals. In a third experiment, a group of 18 month-old (*n*=5; male = 6, female = 4) wildtype and APP/PS1 mice were used to assess the capacity of microglia to respond to inducers of the various activation states *ex vivo*. Mice were anaesthetized and transcardially perfused with sterile PBS prior to sacrifice and removal of brain tissue.

Analysis of BBB permeability by MRI

Magnetic resonance imaging (MRI) was carried out in a small rodent Bruker Biospec system with a 7 Tesla magnet and a 30 cm core (Bruker Biospin, Germany) and extravasation of the gadolinium-based contrast agent gadopentate dimeglumine (Clissmann, Ireland) was used as an indicator of BBB permeability. Anaesthesia was maintained by delivery of a mixture of isoflurane and oxygen (1.5 – 2 % at 1 litre/minute of 100% oxygen); respiration rates and body temperature were monitored throughout the experiment. The right lateral tail vein was cannulated to allow for both pre- and post-contrast measurements to be determined within the same contrast scan without disturbing the animal. Contrast imaging was carried out using a 10 repetition T1-weighted fast low angle shot (FLASH) sequence (1 repetition time: 2 minutes, 11 seconds), with the 15 slice protocol having dimensions of 128 x 128 voxels per slice. Pre-contrast measurements (baseline) were acquired on the first repetition of the scan and the contrast agent was injected via the tail vein cannula at the beginning of the second repetition. Gadolinium-enhanced contrast images were analysed using Medical Image Processing, Analysis, and Visualization (MIPAV) software, with the average signal intensity changes in each treatment group plotted against repetition. Anatomically-distinct regions of interest viewed in the first repetition were overlaid with a 2 x 2 voxel square, and average pre-contrast intensity measured. Values for each data set were normalized to the pre-contrast measurement and expressed relative to the pre-contrast value.

Immunohistochemistry for fibrinogen

Cryostat sections from wildtype and APP/PS1 and mice were prepared for immunohistochemistry as previously described (Kelly *et al*., 2013). Briefly, sections were fixed in ice-cold methanol, washed (PBS containing 0.02% Triton X-100™) and blocked with 10% normal goat serum/4% bovine serum albumin in wash buffer. Sections were incubated with rabbit–anti-human fibrinogen antibody (1:100 in block buffer; Dako, USA), reported to cross-react with murine tissue, overnight at 4°C. Sections were washed, incubated with Alexa Fluor® 488 goat anti-rabbit secondary IgG (1:4000; Invitrogen, UK) and mounted onto glass slides (Vectashield® with DAPI; Vector Laboratories, UK). Images were acquired using a LSM 510 Confocal Laser Scanning Microscope and visualized using LSM Image Browser Rel. 4.2.

Detection of SDS- and guanidine-soluble Aβ

Snap-frozen hippocampal tissue was homogenized in sodium dodecyl sulfate (SDS) buffer (1% SDS, 50mM NaCl in dH_2O) containing protease and phosphatase inhibitors (1%; Sigma-Aldrich, UK) and centrifuged at 21,500 x *g* for 20 minutes at 4°C. SDS-soluble Aβ was assessed in the supernatants while guanidine-soluble Aβ was extracted from the pellets (50mM Tris-HCl, 5M guanidine in dH_2O). Aβ concentrations were determined using a MULTI-SPOT® Human/Rodent (4G8) Abeta Triplex Ultra-Sensitive Assay (Meso Scale Discovery, USA) as per the manufacturer's instructions. The plate was read using a Mesoscale Sector Imager (Meso Scale Discovery, USA) and Aβ concentrations calculated relative to the standard curve and expressed as ng/mg total protein.

Analysis of mRNA expression by real-time PCR

RNA was isolated from cortical tissue using a Nucleospin® RNAII kit (Macherey-Nagel GmbH, Germany) and reverse transcribed into cDNA using a High-Capacity cDNA Archive kit (Applied Biosystems, UK) as per manufacturer's instructions. Assay ID's for the genes examined were as follows: β-actin (4352341E), CD68 (Mm03047340_m1), CD11b (Mm00434455_m1), TNFα (Mm00443258_m1), IL-1β (Mm00434228_m1), mannose receptor (MRC1; Mm00485148_m1), brain

derived neurotrophic factor (BDNF; Mm04230607_s1), nerve growth factor (NGF; Mm00443039_m1) and macrophage inflammatory protein (MIP)-1α (Mm00441258_m1). Real-time PCR was performed using an ABI Prism 7300 instrument (Applied Biosystems, UK) with β-actin as the endogenous control. Relative gene expression was calculated using the ΔΔCT method with Applied Biosystems RQ software (Applied Biosystems, UK).

Analysis of IL-10, CXCL1 and IFNγ concentrations by Multiplex ELISA

IL-10, CXCL1 and IFNγ concentrations were assessed in hippocampal homogenate using a Mouse ProInflammatory 7-Plex Ultra-Sensitive as per manufacturer's instructions (Meso Scale Discovery, USA). Concentrations were calculated relative to the appropriate standard curve and expressed as pg/mg protein.

Cell isolation from brain tissue by density centrifugation

Stock isotonic Percoll was obtained by mixing nine volumes of Percoll (Sigma-Aldrich, UK) with one volume of 10X PBS. Further Percoll gradients were prepared with 1X PBS as appropriate. Following sacrifice, brain tissue was dissected and placed in 1X HBSS (Invitrogen, UK), cross-chopped, homogenized and triturated using fire-polished Pasteur pipettes with three decreasing diameters. Cell suspensions were filtered through a cell strainer (70μM) and cells pelleted by centrifugation. The resultant pellets were re-suspended in 75% Percoll (10ml) and overlaid with 25% Percoll (10ml) and 1X PBS (6ml) and centrifuged at 800 x *g* for 30 minutes at 4°C. Following centrifugation, an enriched microglial population was collected from the 25-75% interface (de Haas *et al*., 2007). The purity of isolated $CD11b^+$ microglia was 60-70%, as assessed by flow cytometry. Cells were removed, washed and resuspended in FACS buffer (2% FBS, 0.1% NaN_3 in PBS) for flow cytometry or RPMI (Invitrogen, UK) and stimulated with IFNγ (100ng/ml) or IL-4/IL-13 (10ng/ml each) for 1 hour prior to analysis of intracellular signaling proteins. For detection of infiltrating cells, brain tissue was prepared as above, resuspended in 70% Percoll (9ml), underlaid with 100% Percoll (5ml) and overlaid with 57% Percoll (9ml), 21.5% Percoll (9ml) and 1X PBS (9ml). The gradient was centrifuged at

1250 x *g* for 45 minutes at 4°C and mononuclear cells were collected from the 57-70% and 21.5-57% interfaces for flow cytometry.

Analysis of intracellular signaling proteins by Western immunoblotting

Hippocampal tissue and enriched microglial preparations stimulated *ex vivo* with IFNγ or IL-4/IL-13 were assessed for protein expression by electrophoresis and Western immunoblotting as previously described (Minogue *et al*., 2012). Primary antibodies against pSTAT1 (1:1000; Cell Signaling Technology, USA) and pSTAT6 (1:1000; Merck Millipore, USA) were used with horseradish peroxidise-conjugated secondary antibodies (1:5000; Jackson ImmunoResearch, UK). Bands were visualized using Supersignal West Pico Chemiluminescent Substrate (Thermo Scientific, USA) and images were captured using a Fujifilm LAS-3000 (Brennan & Co., Ireland).

Assessment of receptor expression, infiltrating cells and phagocytosis by flow cytometry

Flow cytometry was carried out as previously described (Jones *et al*., 2013), with the exception that cells were blocked in FACS buffer containing purified anti-mouse CD16/CD32 (1:100; BD Biosciences, UK). Antibodies used for analysis of microglia were Alexa Fluor 647 anti-mouse CD11b (1:100; BD Biosciences, UK), PE anti-mouse IL-4Rα (1:100; R&D Systems, UK), PerCP anti-mouse IL-10Rβ (1:100; R&D Systems, UK) and PE anti-mouse IFNγR (1:100; eBioscience, UK). Infiltrating monocytes/macrophages and neutrophils were identified by staining for PE-Cy7 anti-mouse CD45 (1:100, Bioscience, UK), Alexa Fluor 647 anti-mouse CD11b (1:100; BD Biosciences, UK) and FITC anti-mouse Ly6G (1:100; BioLegend, UK), and these cells were identified as $CD11b^{+}CD45^{hi}$ and $CD11b^{+}Ly6G^{+}$ respectively. Immunofluorescence was read immediately on a DAKO CyAn-ADP 7 colour flow cytometer with Summit software v4.3 for acquisition. BD™ CompBeads (BD Bioscience, UK) were used to optimise fluorescence settings and further flow cytometric analysis was carried out in FlowJo v7.6.5. Unstained cells and fluorescence minus one (FMO) tubes were used to gate the percentage of positive cells in any channel.

Results

Increased Aβ burden is associated with enhanced microglial activation and markers of classical activation in 24 month-old APP/PS1 mice.

Accumulation of Aβ occurs in APP/PS1 mice from as early as 5 months of age (Jankowsky *et al*., 2004) with evidence from this laboratory identifying marked changes in 7-8 month-old APP/PS1 animals (O'Reilly and Lynch, 2012, Gallagher *et al*., 2013). The data presented here demonstrate that concentrations of SDS- and guanidine-soluble Aβ were enhanced in hippocampal tissue prepared from 14 and 24 month-old APP/PS1, compared with wildtype, mice ($^{***}p<0.001$; 2-way ANOVA; Table 1), and that this increase was significantly greater in 24 month-old, compared with 14 month-old, animals ($^{+}p<0.05$; $^{++}p<0.01$, $^{+++}p<0.001$: 2-way ANOVA; Table 1).

One apparently anomalous finding is that activated glial cells surround Aβ plaques in the AD brain and in mouse models of AD, yet Aβ accumulation continues, suggesting that the phagocytic function of these cells is compromised. Here we assessed expression of CD68, a lysosomal protein which is upregulated in phagocytic cells (Zotova *et al*., 2011) and show that CD68 mRNA was significantly increased in tissue prepared from APP/PS1, compared with wildtype, mice ($^{***}p<0.001$; 2-way ANOVA; Figure 1A), and that expression was greater in tissue from 24 month-old, compared with 14 month-old, mice ($^{+}p<0.05$: 2-way ANOVA; Figure 1A). Expression of CD11b, TNFα and IL-1β are indicative of classical activation of microglia (Colton and Wilcock, 2010) and all were found to be increased in hippocampal tissue prepared from APP/PS1, compared with wildtype, mice ($^{**}p<0.01$; $^{***}p<0.001$; 2-way ANOVA; Figure 1B, C and D); an effect that was enhanced in 24 month-old APP/PS1 mice ($^{+}p<0.05$; ANOVA; Figure 1B, C and D).

IFNγ signaling is enhanced in 24 month-old APP/PS1 mice.

Classical activation is stimulated by the interaction of IFNγ with its receptor and we demonstrate that IFNγ concentration was greater in tissue prepared from APP/PS1, compared with wildtype, mice

($^{**}p<0.01$; 2-way ANOVA; Figure 2A) and in 24 month-old, compared with 14 month-old, mice ($^{###,+++}p<0.001$; 2-way ANOVA; Figure 2A). IFNγ-induced signaling requires recruitment and activation of STAT1, which becomes phosphorylated, dimerises and translocates to the nucleus where it upregulates transcription of a number of genes associated with proinflammatory signaling. Expression of phosphorylated STAT1 was increased in hippocampal lysates prepared from 24 month-old APP/PS1 mice compared with all other cohorts ($^{**}p<0.01$; 2-way ANOVA; Figure 2B), whereas total STAT1 expression was unchanged in hippocampal tissue from all groups (data not shown). Furthermore, the expression of IFNγ receptor (IFNγR) was significantly upregulated on $CD11b^+$ cells isolated from brain tissue of APP/PS1, compared with wildtype, mice ($^{**}p<0.01$; 2-way ANOVA; Figure 2C). To confirm that microglia from APP/PS1 mice have a greater capacity to respond to IFNγ, an enriched microglial population was isolated from brain tissue of wildtype and APP/PS1 mice and stimulated with IFNγ for 1 hour *ex vivo*. Expression of pSTAT1 was significantly increased in microglia isolated from both wildtype and APP/PS1 mice ($^{***}p<0.001$; 2-way ANOVA; Figure 2D) however this effect was more pronounced in microglia isolated from APP/PS1 mice ($^{+++}p<0.001$; 2-way ANOVA; Figure 2D).

Markers of alternative activation are unchanged in APP/PS1 mice

In contrast to the evidence indicating that microglia in APP/PS1 mice adopt a classically-activated phenotype, there was no age- nor genotype-associated change in mRNA expression of MRC1 (Figure 3A), arginase-1 or FIZZ-1 (data not shown) all of which are markers of alternative activation. MRC1 was detected on $CD11b^+$ cells (Figure 3B) with no genotype-related change observed. MRC1 expression was also detected on $CD11b^-$ cells, although to a lesser extent, as well as on $CD11b^+CD45^{hi}$ monocytes/macrophages (data not shown). Anti-inflammatory cytokines such as IL-4 induce alternative activation (Colton and Wilcock, 2010) and expression of the IL-4 receptor (IL-4R) was significantly decreased on $CD11b^+$ cells prepared from 24 month-old, compared with 14 month-old, mice ($^{*}p<0.05$; 2-way ANOVA; Figure 3C). This was accompanied by a decrease in the IL-4-associated signaling molecule pSTAT6, although this did not reach statistical significance (Figure

3D). Microglia prepared from wildtype and APP/PS1 mice were incubated in the presence or absence of IL-4/IL-13 and expression of pSTAT6 assessed. The data show that IL-4/IL-13 enhanced phosphorylation of STAT6 in microglia isolated from both wildtype and APP/PS1 mice, however no genotype-related difference was observed ($^{***}p<0.001$; 2-way ANOVA; Figure 3E).

Markers of microglial deactivation are decreased in APP/PS1 mice

Macrophages, in response to IL-10 or TGFβ, adopt a deactivated phenotype (Gordon, 2003) and a similar state in microglia has been described (Colton and Wilcock, 2010). Hippocampal IL-10 concentration was greater in tissue prepared from APP/PS1, compared with wildtype, mice ($^{**}p<0.01$; 2-way ANOVA; Figure 4A), however there was an age-related decrease in cytokine concentration in APP/PS1 mice ($^{++}p<0.01$; 2-way ANOVA; Figure 4A) and the number of $CD11b^+$ cells expressing the IL-10R was significantly decreased in 24 month-old, compared with 14 month-old, mice ($^{*}p<0.05$; ANOVA; Figure 4B). Expression of BDNF and NGF mRNA was decreased in tissue prepared from APP/PS1, compared with wildtype, mice ($^{*}p<0.05$; $^{**}p<0.01$; 2-way ANOVA; Figure 4C, D) reflecting a genotype-related decrease in markers of deactivation. Thus the data describe a shift towards a classical, proinflammatory microglial phenotype in APP/PS1 mice and an apparent age-related dysregulation in mechanisms designed to maintain homeostasis.

Increased numbers of infiltrating immune cells are present in brains of APP/PS1 mice

IFNγ is generally not considered to be produced by cells resident in the CNS but by peripheral immune cells such as macrophages, neutrophils and T cells. Here, we demonstrate an increase in $CD11b^+CD45^{hi}$ monocytes/macrophages and $CD11b^+Ly6G^+$ neutrophils in brain tissue prepared from APP/PS1, compared with wildtype, mice ($^{**}p<0.01$; Student's *t*-test for independent means; Figure 5A, B). Since these cells are capable of producing and releasing IFNγ, they may provide the trigger which drives microglia towards a classically-activated phenotype in APP/PS1 mice.

BBB permeability and chemokine expression are increased in APP/PS1 mice

To examine possible mechanisms by which peripheral immune cells enter the brain, we first evaluated BBB permeability by MRI in 14 and 24 month-old wildtype and APP/PS1 mice and show an age-related increase in signal intensity (SI) in all areas of the brain examined in wildtype mice ($^{\#\#}p<0.01$; 2-way ANOVA; Figure 6A-C). A marked increase in BBB permeability was observed in APP/PS1, compared with wildtype, mice ($^{***}p<0.001$; 2-way ANOVA; Figure 6A, B and C) and BBB permeability in the hippocampus was increased in 24 month-old, compared with 14 month-old, APP/PS1 mice ($^{+}p<0.05$; 2-way ANOVA; Figure 6A-C). Indeed the effect of age on BBB was more pronounced in wildtype, than in APP/PS1, mice but this may be a consequence of the existing genotype-related increase in gadolinium extravasation in 14 month-old mice. Overall, the present findings concur with the evidence that Aβ causes vascular disruption and enhances BBB permeability (Thomas *et al*., 1997, Ryu and McLarnon, 2009), promoting transendothelial migration of leukocytes (Gonzalez-Velasquez and Moss, 2008, Rossi *et al*., 2011). As an additional method of evaluating BBB permeability, brain sections from wildtype and APP/PS1 mice were assessed for immunoreactivity of the serum-derived protein fibrinogen (MW = 340,000 Da). Previous studies have demonstrated that molecules such as thrombin and fibrinogen can freely enter and accumulate in the brain across a damaged BBB (Bell *et al*., 2010). Representative images (Figure 6D) demonstrate increased fibrinogen immunoreactivity in the hippocampus of APP/PS1, compared with wildtype, mice and thus these data concur with those obtained by assessing gadolinium extravasation.

Enhanced BBB permeability may be sufficient to allow infiltration of peripheral immune cells, however a second mechanism which facilitates entry of these cells into the brain could be through development of a chemotactic gradient. Interestingly, we observed a marked increase in mRNA expression of MIP-1α in hippocampal tissue prepared from APP/PS1, compared with wildtype, mice ($^{***}p<0.01$; ANOVA; Figure 7A). Similar changes were also observed in RANTES, IP-10 and MCP-1 expression, although these did not reach statistical significance (data not shown). CXCL1 concentration was increased in tissue from 24 month-old, compared with 14 month-old, mice

(**p<0.01; 2-way ANOVA; Figure 7B) and a genotype-related increase was observed in older animals (+p<0.05; 2-way ANOVA; Figure 7B).

Discussion

Inflammation is recognized as an important facet of neurodegenerative disease, however the underlying causes and consequences remain to be clarified. Here, we sought to delineate the differences in microglial activation states between normal aging and those associated with disease progression in a mouse model of AD. We have identified a shift in microglial activation towards a classical, proinflammatory phenotype, with a concomitant decrease in expression of molecules associated with deactivation and cellular repair in aged APP/PS1 mice. We propose that this state is reinforced by infiltration of immune cells, capable of producing IFNγ, that occurs as a result of enhanced BBB permeability and a developing chemotactic gradient.

It has recently been suggested that microglia, like macrophages, can be categorized into at least three broad phenotypes termed classical, alternative and acquired deactivation states (Martinez *et al*., 2009), induced by cytokines such as IFNγ, IL-4 and IL-10 respectively. Several markers of microglial activation were upregulated in an age-dependent manner in the hippocampus of APP/PS1 mice, including CD11b and CD68. Genotype-related increases in these markers have been reported (Gallagher *et al*., 2012) and the present findings support and extend these observations to show that microglial activation continues to develop with age, paralleling the increase in Aβ accumulation.

Interestingly, the ability of activated microglia from APP/PS1 mice to phagocytose fluorescently-labeled latex beads was unchanged in comparison to their wildtype counterparts (data not shown), although this may not necessarily reflect their ability to phagocytose Aβ. It has been reported that Th1 cytokines inhibit microglial phagocytosis of Aβ, whereas IL-4 and IL-10 have the opposite effect (Koenigsknecht-Talboo and Landreth, 2005). Knockout of IFNγR1 in APP mice is associated with

reduced Aβ deposition in the cortex and hippocampus which correlates with decreased gliosis (Yamamoto *et al*., 2007). In contrast, overexpression of IFNγ in TgCRND8 mice has been shown to upregulate glial activation, specifically molecules associated with classical activation, enhance monocyte infiltration and attenuate plaque deposition through enhanced phagocytosis (Chakrabarty *et al*., 2010). Furthermore, alternative activation of microglia in APP/PS1 mice, induced by the PPARγ activator pioglitazone (Mandrekar-Colucci *et al*., 2012) or NLRP3 knockdown (Heneka *et al*., 2013) was associated with an increase in Aβ clearance. While recent evidence has indicated that microglia surrounding Aβ deposits in APP/PS1 mice may be alternatively activated and those distal to the deposits are classically activated in older animals (Jimenez *et al*., 2008), the effect of activation state on the capacity of microglia to phagocytose Aβ remains to be clarified. In the context of AD in particular, it is important to unravel the factors that contribute to the apparent inability of microglia to phagocytose Aβ despite the proximity of activated cells to the Aβ-containing plaques.

We demonstrate that microglia adopt a classically-activated phenotype in the brains of APP/PS1 mice which progresses with age; indeed it appears that mechanisms designed to limit the proinflammatory response are dysfunctional. Specifically, markers of the alternative or deactivated states were either unchanged or decreased with age and genotype, and expression of IL-4R and IL-10R was decreased on $CD11b^+$ cells. IL-10 and IL-4 have been shown to suppress astrogliosis and microgliosis in APP/PS1 mice (Kiyota *et al*., 2012) and inhibit the Aβ-induced production of proinflammatory cytokines by glial cells *in vitro* (Szczepanik *et al*., 2001). In TgCRND8 mice that received adenoviral delivery of IL-10, hippocampal-dependent spatial learning and neurogenesis were improved while Aβ deposition/burden was unaffected (Kiyota *et al*., 2012). IL-10, like TGFβ, triggers acquired deactivation of microglia and enhanced expression of NGF is associated with this state (Wei and Jonakait, 1999, Colton and Wilcock, 2010). The data presented here demonstrate that neurotrophin expression was decreased in the hippocampus of APP/PS1, compared with wildtype, mice. NGF represses the costimulatory molecule CD40 in cultured rat microglia indicating that it may play a role in immune cell/microglial interactions (Noga *et al*., 2007) and both NGF and BDNF are capable of

inducing release of IL-10 from dendritic cells while having no effect on IL-6 (Wei and Jonakait, 1999). Taken together, these data imply that NGF and BDNF are associated with resolution of inflammation. Additionally, the pronounced declines in BDNF and NGF might be of particular functional consequence, as both are critical for facilitating synaptic plasticity, learning and memory which are impaired with age and in APP/PS1 mice (Gooney *et al*., 2004, Kelly *et al*., 2013).

We found no evidence of any change in markers of alternative activation with age or genotype although expression of the IL-4R was decreased on $CD11b^+$ cells in older mice, accompanied by a similar reduction in expression of phosphorylated STAT6. IL-4 has been shown to attenuate AD pathogenesis by reducing gliosis and Aβ deposition in APP/PS1 mice (Kiyota *et al*., 2010) and therefore the loss of IL-4-induced signaling described here may contribute to the enhanced proinflammatory state. Overall, the evidence indicates a shift towards a proinflammatory phenotype in aged APP/PS1 that is likely to be exacerbated by downregulation of IL-4- and IL-10-driven modulation.

The trigger for classical activation is IFNγ, concentration of which was increased in hippocampus of APP/PS1 mice and exacerbated with age, paralleling the increased expression of markers of classical activation, IL-1β, TNFα and CD11b (Colton, 2009). The evidence suggests that microglial sensitivity to IFNγ was increased in APP/PS1 mice since there was a genotype-related upregulation of IFNγR on $CD11b^+$ cells and an increase in phosphorylated STAT1. This enhanced responsiveness was specific to IFNγ since IL-4/IL-13-induced phosphorylation of STAT6 was not affected by genotype. These data imply that microglia in APP/PS1 mice are primed to respond to IFNγ and, as a consequence, adopt the classically-activated phenotype with age. While IFNγ has not yet been reported to be increased in AD brain, many IFNγ-responsive genes are upregulated (Colangelo *et al*., 2002, Ricciarelli *et al*., 2004) and expression of STAT1 has been shown to be enhanced in temporal cortex of AD brains (Kitamura *et al*., 1997).

As IFNγ is not usually produced by cells of the CNS, we considered that the observed increase in IFNγ in the brains of APP/PS1 mice might result from infiltration of IFNγ-producing cells. Analysis of brain tissue by flow cytometry identified marked genotype-related increases in the infiltration of macrophages and neutrophils. These cells may enter the brain in response to a chemotactic signal and the data indicate that expression of several chemokines was increased in a genotype- and age-dependent manner, particularly MIP-1α and CXCL1. MIP-1α serves to attract macrophages and T cells into the CNS (Zang *et al*., 2000, Fife *et al*., 2001, Cardona *et al*., 2003), whereas CXCL1 is a potent chemoattractant for neutrophils and is upregulated in macrophages in response to inflammatory stimuli including LPS (Rovai *et al*., 1998). Several groups have reported the presence of peripheral immune cells in animal models of AD (Town *et al*., 2008, Browne *et al*., 2013), as well as in the brain parenchyma of patients suffering from AD (Togo *et al*., 2002).

An intact BBB provides an important protective strategy for limiting the entry of cells into the brain. Significantly, we have identified a genotype-related increase in BBB permeability as assessed by gadolinium extravasation and this effect was exacerbated with age. Numerous vascular abnormalities are found in the AD brain including alterations in smooth muscle cells and pericytes, endothelial cell thinning, loss of endothelial mitochondria and thickening of the vascular basement membrane (Stewart *et al*., 1992, Kalaria, 1996, Vinters *et al*., 1996, Kalaria and Ballard, 1999). AD has also been associated with increased vascular permeability and protein extravasation in the brain parenchyma (Eikelenboom and Stam, 1982, Mann, 1982, Wisniewski and Kozlowski, 1982). More recently, Aβ has been demonstrated to contribute to BBB leakage in a mouse model of cerebral amyloid angiopathy (CAA) as well as in patients with CAA (Hartz *et al*., 2012). Several studies have linked cytokine secretion, including IL-1β, to BBB disruption (de Vries *et al*., 1996). Data from this study indicate that changes in IL-1β and TNFα parallel those observed in BBB permeability. Whereas brain endothelial cells respond to inflammatory cytokines under control conditions, during pathological conditions cytokines dysregulate the barrier-forming cells indirectly through astrocyte activation resulting in reorganization of junctions, matrix, focal adhesion or release of barrier-modulating factors

including matrix metalloproteases (Chaitanya *et al*., 2012). Whether Aβ impacts directly on the neurovascular unit through alteration of tight junction protein expression to increase BBB permeability or whether this occurs as a result of the inflammatory microenvironment remains to be determined, however the present data demonstrate a tight coupling between these factors.

It has been proposed that microglia become dysfunctional with age and may lose their neuroprotective properties leading to chronic neurodegeneration, however this concept is based on morphological, rather than functional, changes. The data from this study indicate that microglia are not less active with age but alter their phenotype; indeed the changes observed in the deactivation state appear to relate to aging rather than disease pathology since these changes were also apparent in older wildtype mice. Here, the effect of the Aβ stimulus, driven through overexpression of APP and PS1, on microglia is compounded as animals age and it may explain, in part, why certain individuals bearing Aβ load progress to AD while others do not. This is consistent with the interpretation that aging primes microglia which then respond to AD pathology. Recent evidence has highlighted involvement of neuroinflammation in preclinical stages of AD and that this occurs prior to cognitive decline. If immune and inflammation-related genes are activated in the brain in the course of normal aging, it is possible that such neuroinflammation primes the brain for cognitive decline, neurodegenerative cascades and progression to AD.

Figure Legends

Figure 1. Enhanced microglial activation and markers of classical inflammation in 24 month-old APP/PS1 mice.

CD68 (A) and CD11b (B) mRNA expression were significantly enhanced in APP/PS1, compared with wildtype, mice ($^{***}p<0.001$; 2-way ANOVA), and this effect was exacerbated in 24 month-old animals ($^{+}p<0.05$; 2-way ANOVA). TNFα (C) and IL-1β (D) mRNA expression were significantly increased in hippocampal tissue prepared from APP/PS1, compared with wildtype, mice ($^{**}p<0.01$;

$^{***}p<0.001$; 2-way ANOVA) and further enhanced in 24 month-old, compared with 14 month-old, APP/PS1 mice ($^{+}p<0.05$; 2-way ANOVA). Data are expressed as means ± SEM.

Figure 2. IFNγ signaling is enhanced in 24 month-old APP/PS1 mice.

Hippocampal concentration of IFNγ (A) was significantly greater in tissue prepared from APP/PS1, compared with wildtype, mice ($^{**}p<0.01$; 2-way ANOVA) and in tissue prepared from 24 month-old, compared with 14 month-old, APP/PS1 mice ($^{+++}p<0.001$; 2-way ANOVA). An age-related increase in IFNγ was also observed in wildtype mice ($^{\#\#\#}p<0.001$; 2-way ANOVA). Expression of phosphorylated STAT1 (B) was enhanced in 24 month-old APP/PS1 mice compared with all other groups ($^{**}p< 0.01$; 2-way ANOVA). Expression of IFNγR (C) was increased on $CD11b^{+}$ cells isolated from brain tissue of APP/PS1, compared with wildtype, mice ($^{**}p< 0.01$; 2-way ANOVA). Following stimulation with IFNγ *ex vivo*, expression of phosphorylated STAT1 (D) was increased in enriched microglial populations isolated from wildtype and APP/PS1 mice ($^{***}p<0.001$; 2-way ANOVA), this effect was significantly greater in APP/PS1, compared with wildtype, microglia ($^{+++}p<0.001$; 2-way ANOVA). ND = not detected. Data are expressed as mean ± SEM.

Figure 3. Markers of alternative activation are unchanged in APP/PS1 mice.

MRC1 mRNA expression (A) was unaffected by age or genotype. MRC1 (B) was similarly expressed on $CD11b^{+}$ cells isolated from brain tissue of wildtype and APP/PS1 mice. Expression of IL-4R (C) was decreased on $CD11b^{+}$ cells isolated from brain tissue of 24 month-old, compared with 14 month-old, mice ($^{*}p< 0.05$; 2-way ANOVA). No effect of genotype was observed. Expression of phosphorylated STAT6 (D) showed a similar pattern to the expression of IL-4R on $CD11b^{+}$ cells. Following stimulation with IL-4/IL-13 *ex vivo*, expression of phosphorylated STAT6 (E) was increased in enriched microglial populations isolated from wildtype and APP/PS1 mice ($^{***}p< 0.001$; 2-way ANOVA). No effect of genotype was observed. ND = not detected. Data are expressed as mean ± SEM.

Figure 4. Markers of microglial deactivation are decreased in APP/PS1 mice.

Hippocampal concentration of IL-10 (A) was significantly greater in tissue prepared from APP/PS1, compared with wildtype, mice ($^{**}p<0.01$; 2-way ANOVA), however this effect was less profound in 24 month-old APP/PS1 mice ($^{++}p<0.01$; 2-way ANOVA). Expression of IL-10R (B) was decreased on $CD11b^{+}$ cells isolated from brain tissue of 24 month-old, compared with 14 month-old, mice ($^{*}p< 0.05$; 2-way ANOVA). BDNF (C) and NGF (D) mRNA expression were significantly decreased in tissue prepared from APP/PS1, compared with wildtype, mice ($^{*}p<0.05$; $^{**}p<0.01$; 2-way ANOVA). Data are expressed as mean ± SEM.

Figure 5. Increased numbers of infiltrating immune cells in brains of APP/PS1 mice.

The number of $CD11b^{+}CD45^{hi}$ cells (A; monocytes/macrophages) and $CD11b^{+}Ly6G^{+}$ cells (B; neutrophils) were significantly increased in brains of APP/PS1, compared with wildtype, mice ($^{**}p<0.01$; Student's *t*-test for Independent means). Representative FACS plots are shown and data are expressed as mean ± SEM.

Figure 6. BBB permeability is increased in APP/PS1 mice.

Gadolinium-enhanced contrast imaging was used to assess permeability of BBB in wildtype and APP/PS1 mice. Gadolinium was injected at the commencement of repetition 2. Mean SI was increased in the left dentate gyrus (A) and CA1 (B) of APP/PS1, compared with wildtype, mice ($^{***}p<0.01$; 2-way ANOVA), this effect was exacerbated in 24 month-old, compared with 14 month-old, APP/PS1 mice ($^{+}p<0.05$; 2-way ANOVA). Mean SI was increased in the left dentate gyrus (A) and CA1 (B) of 24 month-old, compared with 14 month-old, wildtype mice ($^{\#\#}p<0.01$; 2-way ANOVA). Values are presented as a proportion of the pre-contrast measure (repetition 1) and are means ± SEM. Representative contrast MRI data sets from 14 and 24 month-old wildtype and APP/PS1 mice injected with gadolinium are shown in (C). Fibrinogen (D; green) staining was increased in the hippocampus of APP/PS1, compared with wildtype, mice. Nuclei were counterstained using DAPI (blue). Scale bars at 50μM. Data are expressed as mean ± SEM.

Figure 7. Chemokine expression is increased in APP/PS1 mice.

MIP-1α mRNA (A) expression was increased in 24 month-old APP/PS1, compared with all other cohorts of mice ($^{***}p<0.001$; 2-way ANOVA). Hippocampal CXCL1 (B) protein concentration was increased in 24 month-old, compared with 14 month-old, mice ($^{**}p<0.01$; 2-way ANOVA), this effect was enhanced in 24 month-old APP/PS1 mice ($^{+}p<0.05$; 2-way ANOVA). Data are expressed as mean ± SEM.

Figure 8. Age-associated dysregulation of microglial activation is coupled with enhanced BBB permeability and pathology in APP/PS1 mice

Aging and Aβ burden are associated with increased classical (M1) and decreased alternative and acquired deactivation (M2) in APP/PS1 mice. We hypothesize that these changes result in disruption of the BBB and, in tandem with an enhanced chemokine profile, this permits infiltration of IFNγ-producing cells into the brain parenchyma serving to reinforce the M1 phenotype of microglia through their enhanced responsiveness to IFNγ.

Table Legends

Table 1. Aβ burden is increased with age in APP/PS1 mice

Concentrations of SDS- and guanidine-soluble $A\beta_{1-40}$ and $A\beta_{1-42}$ were significantly increased in hippocampal tissue prepared from APP/PS1, compared with wildtype, mice ($^{***}p<0.001$; 2-way ANOVA). Aβ burden was greater in hippocampal tissue prepared from 24 month-old, compared with 14 month-old, APP/PS1 mice ($^{+}p<0.05$, $^{++}p<0.01$, $^{+++}p<0.001$; 2-way ANOVA). Data are presented as ng Aβ/mg total protein and expressed as means ± SEM.

References

Avison MJ, Nath A, Greene-Avison R, Schmitt FA, Bales RA, Ethisham A, Greenberg RN, Berger JR (2004) Inflammatory changes and breakdown of microvascular integrity in early human immunodeficiency virus dementia. J Neurovirol 10:223-232.

Bell RD, Winkler EA, Sagare AP, Singh I, LaRue B, Deane R, Zlokovic BV (2010) Pericytes control key neurovascular functions and neuronal phenotype in the adult brain and during brain aging. Neuron 68:409-427.

Borchelt DR, Thinakaran G, Eckman CB, Lee MK, Davenport F, Ratovitsky T, Prada CM, Kim G, Seekins S, Yager D, Slunt HH, Wang R, Seeger M, Levey AI, Gandy SE, Copeland NG, Jenkins NA, Price DL, Younkin SG, Sisodia SS (1996) Familial Alzheimer's disease-linked presenilin 1 variants elevate Abeta1-42/1-40 ratio in vitro and in vivo. Neuron 17:1005-1013.

Browne TC, McQuillan K, McManus RM, O'Reilly JA, Mills KH, Lynch MA (2013) IFN-gamma Production by amyloid beta-specific Th1 cells promotes microglial activation and increases plaque burden in a mouse model of Alzheimer's disease. J Immunol 190:2241-2251.

Cardona AE, Gonzalez PA, Teale JM (2003) CC chemokines mediate leukocyte trafficking into the central nervous system during murine neurocysticercosis: role of gamma delta T cells in amplification of the host immune response. Infect Immun 71:2634-2642.

Chaitanya GV, Cromer W, Wells S, Jennings M, Mathis JM, Minagar A, Alexander JS (2012) Metabolic modulation of cytokine-induced brain endothelial adhesion molecule expression. Microcirculation 19:155-165.

Chakrabarty P, Ceballos-Diaz C, Beccard A, Janus C, Dickson D, Golde TE, Das P (2010) IFN-gamma promotes complement expression and attenuates amyloid plaque deposition in amyloid beta precursor protein transgenic mice. J Immunol 184:5333-5343.

Citron M, Westaway D, Xia W, Carlson G, Diehl T, Levesque G, Johnson-Wood K, Lee M, Seubert P, Davis A, Kholodenko D, Motter R, Sherrington R, Perry B, Yao H, Strome R, Lieberburg I, Rommens J, Kim S, Schenk D, Fraser P, St George Hyslop P, Selkoe DJ (1997) Mutant presenilins of Alzheimer's disease increase production of 42-residue amyloid beta-protein in both transfected cells and transgenic mice. Nat Med 3:67-72.

Colangelo V, Schurr J, Ball MJ, Pelaez RP, Bazan NG, Lukiw WJ (2002) Gene expression profiling of 12633 genes in Alzheimer hippocampal CA1: transcription and neurotrophic factor down-regulation and up-regulation of apoptotic and pro-inflammatory signaling. J Neurosci Res 70:462-473.

Colton CA (2009) Heterogeneity of microglial activation in the innate immune response in the brain. J Neuroimmune Pharmacol 4:399-418.

Colton CA, Mott RT, Sharpe H, Xu Q, Van Nostrand WE, Vitek MP (2006) Expression profiles for macrophage alternative activation genes in AD and in mouse models of AD. J Neuroinflammation 3:27.

Colton CA, Wilcock DM (2010) Assessing activation states in microglia. CNS Neurol Disord Drug Targets 9:174-191.

Czeh M, Gressens P, Kaindl AM (2011) The yin and yang of microglia. Dev Neurosci 33:199-209.

de Haas AH, Boddeke HW, Brouwer N, Biber K (2007) Optimized isolation enables ex vivo analysis of microglia from various central nervous system regions. Glia 55:1374-1384.

de Vries HE, Blom-Roosemalen MC, van Oosten M, de Boer AG, van Berkel TJ, Breimer DD, Kuiper J (1996) The influence of cytokines on the integrity of the blood-brain barrier in vitro. J Neuroimmunol 64:37-43.

Duff K, Eckman C, Zehr C, Yu X, Prada CM, Perez-tur J, Hutton M, Buee L, Harigaya Y, Yager D, Morgan D, Gordon MN, Holcomb L, Refolo L, Zenk B, Hardy J, Younkin S (1996) Increased amyloid-beta42(43) in brains of mice expressing mutant presenilin 1. Nature 383:710-713.

Eikelenboom P, Stam FC (1982) Immunoglobulins and complement factors in senile plaques. An immunoperoxidase study. Acta Neuropathol 57:239-242.

Fife BT, Paniagua MC, Lukacs NW, Kunkel SL, Karpus WJ (2001) Selective CC chemokine receptor expression by central nervous system-infiltrating encephalitogenic T cells during experimental autoimmune encephalomyelitis. J Neurosci Res 66:705-714.

Gallagher JJ, Finnegan ME, Grehan B, Dobson J, Collingwood JF, Lynch MA (2012) Modest Amyloid Deposition is Associated with Iron Dysregulation, Microglial Activation, and Oxidative Stress. J Alzheimers Dis 28:147-161.

Gallagher JJ, Minogue AM, Lynch MA (2013) Impaired performance of female APP/PS1 mice in the Morris water maze is coupled with increased Abeta accumulation and microglial activation. Neurodegener Dis 11:33-41.

Gonzalez-Velasquez FJ, Moss MA (2008) Soluble aggregates of the amyloid-beta protein activate endothelial monolayers for adhesion and subsequent transmigration of monocyte cells. J Neurochem 104:500-513.

Gooney M, Messaoudi E, Maher FO, Bramham CR, Lynch MA (2004) BDNF-induced LTP in dentate gyrus is impaired with age: analysis of changes in cell signaling events. Neurobiol Aging 25:1323-1331.

Gordon S (2003) Alternative activation of macrophages. Nat Rev Immunol 3:23-35.

Hartz AM, Bauer B, Soldner EL, Wolf A, Boy S, Backhaus R, Mihaljevic I, Bogdahn U, Klunemann HH, Schuierer G, Schlachetzki F (2012) Amyloid-beta contributes to blood-brain barrier leakage in transgenic human amyloid precursor protein mice and in humans with cerebral amyloid angiopathy. Stroke 43:514-523.

Heneka MT, Kummer MP, Stutz A, Delekate A, Schwartz S, Vieira-Saecker A, Griep A, Axt D, Remus A, Tzeng TC, Gelpi E, Halle A, Korte M, Latz E, Golenbock DT (2013) NLRP3 is activated in Alzheimer's disease and contributes to pathology in APP/PS1 mice. Nature 493:674-678.

Holcomb L, Gordon MN, McGowan E, Yu X, Benkovic S, Jantzen P, Wright K, Saad I, Mueller R, Morgan D, Sanders S, Zehr C, O'Campo K, Hardy J, Prada CM, Eckman C, Younkin S, Hsiao K, Duff K (1998) Accelerated Alzheimer-type phenotype in transgenic mice carrying both mutant amyloid precursor protein and presenilin 1 transgenes. Nat Med 4:97-100.

Ishii K, Ii K, Hasegawa T, Shoji S, Doi A, Mori H (1997) Increased A beta 42(43)-plaque deposition in early-onset familial Alzheimer's disease brains with the deletion of exon 9 and the missense point mutation (H163R) in the PS-1 gene. Neurosci Lett 228:17-20.

Jankowsky JL, Fadale DJ, Anderson J, Xu GM, Gonzales V, Jenkins NA, Copeland NG, Lee MK, Younkin LH, Wagner SL, Younkin SG, Borchelt DR (2004) Mutant presenilins specifically elevate the levels of the 42 residue beta-amyloid peptide in vivo: evidence for augmentation of a 42-specific gamma secretase. Hum Mol Genet 13:159-170.

Jimenez S, Baglietto-Vargas D, Caballero C, Moreno-Gonzalez I, Torres M, Sanchez-Varo R, Ruano D, Vizuete M, Gutierrez A, Vitorica J (2008) Inflammatory response in the hippocampus of PS1M146L/APP751SL mouse model of Alzheimer's disease: age-dependent switch in the microglial phenotype from alternative to classic. J Neurosci 28:11650-11661.

Jones RS, Minogue AM, Connor TJ, Lynch MA (2013) Amyloid-beta-induced astrocytic phagocytosis is mediated by CD36, CD47 and RAGE. J Neuroimmune Pharmacol 8:301-311.

Kalaria RN (1996) Cerebral vessels in ageing and Alzheimer's disease. Pharmacol Ther 72:193-214.

Kalaria RN, Ballard C (1999) Overlap between pathology of Alzheimer disease and vascular dementia. Alzheimer Dis Assoc Disord 13 Suppl 3:S115-123.

Kelly RJ, Minogue AM, Lyons A, Jones RS, Browne TC, Costello DA, Denieffe S, O'Sullivan C, Connor TJ, Lynch MA (2013) Glial Activation in AbetaPP/PS1 Mice is Associated with Infiltration of IFNgamma-Producing Cells. J Alzheimers Dis.

Kitamura Y, Shimohama S, Ota T, Matsuoka Y, Nomura Y, Taniguchi T (1997) Alteration of transcription factors NF-kappaB and STAT1 in Alzheimer's disease brains. Neurosci Lett 237:17-20.

Kiyota T, Ingraham KL, Swan RJ, Jacobsen MT, Andrews SJ, Ikezu T (2012) AAV serotype 2/1-mediated gene delivery of anti-inflammatory interleukin-10 enhances neurogenesis and cognitive function in APP+PS1 mice. Gene Ther 19:724-733.

Kiyota T, Okuyama S, Swan RJ, Jacobsen MT, Gendelman HE, Ikezu T (2010) CNS expression of anti-inflammatory cytokine interleukin-4 attenuates Alzheimer's disease-like pathogenesis in APP+PS1 bigenic mice. FASEB J 24:3093-3102.

Koenigsknecht-Talboo J, Landreth GE (2005) Microglial phagocytosis induced by fibrillar beta-amyloid and IgGs are differentially regulated by proinflammatory cytokines. J Neurosci 25:8240-8249.

Mandrekar-Colucci S, Karlo JC, Landreth GE (2012) Mechanisms underlying the rapid peroxisome proliferator-activated receptor-gamma-mediated amyloid clearance and reversal of cognitive deficits in a murine model of Alzheimer's disease. J Neurosci 32:10117-10128.

Mann DM (1982) Nerve cell protein metabolism and degenerative disease. Neuropathol Appl Neurobiol 8:161-176.

Mann DM, Iwatsubo T, Nochlin D, Sumi SM, Levy-Lahad E, Bird TD (1997) Amyloid (Abeta) deposition in chromosome 1-linked Alzheimer's disease: the Volga German families. Ann Neurol 41:52-57.

Martinez FO, Helming L, Gordon S (2009) Alternative activation of macrophages: an immunologic functional perspective. Annu Rev Immunol 27:451-483.

Minogue AM, Barrett JP, Lynch MA (2012) LPS-induced release of IL-6 from glia modulates production of IL-1beta in a JAK2-dependent manner. J Neuroinflammation 9:126.

Mosser DM (2003) The many faces of macrophage activation. J Leukoc Biol 73:209-212.

Mosser DM, Edwards JP (2008) Exploring the full spectrum of macrophage activation. Nat Rev Immunol 8:958-969.

Noga O, Peiser M, Altenahr M, Knieling H, Wanner R, Hanf G, Grosse R, Suttorp N (2007) Differential activation of dendritic cells by nerve growth factor and brain-derived neurotrophic factor. Clin Exp Allergy 37:1701-1708.

O'Reilly JA, Lynch M (2012) Rosiglitazone Improves Spatial Memory and Decreases Insoluble Abeta(1-42) in APP/PS1 Mice. J Neuroimmune Pharmacol 7:140-144.

Ricciarelli R, d'Abramo C, Massone S, Marinari U, Pronzato M, Tabaton M (2004) Microarray analysis in Alzheimer's disease and normal aging. IUBMB Life 56:349-354.

Rossi B, Angiari S, Zenaro E, Budui SL, Constantin G (2011) Vascular inflammation in central nervous system diseases: adhesion receptors controlling leukocyte-endothelial interactions. J Leukoc Biol 89:539-556.

Rovai LE, Herschman HR, Smith JB (1998) The murine neutrophil-chemoattractant chemokines LIX, KC, and MIP-2 have distinct induction kinetics, tissue distributions, and tissue-specific sensitivities to glucocorticoid regulation in endotoxemia. J Leukoc Biol 64:494-502.

Ryu JK, McLarnon JG (2009) A leaky blood-brain barrier, fibrinogen infiltration and microglial reactivity in inflamed Alzheimer's disease brain. J Cell Mol Med 13:2911-2925.

Scheuner D, Eckman C, Jensen M, Song X, Citron M, Suzuki N, Bird TD, Hardy J, Hutton M, Kukull W, Larson E, Levy-Lahad E, Viitanen M, Peskind E, Poorkaj P, Schellenberg G, Tanzi R, Wasco W, Lannfelt L, Selkoe D, Younkin S (1996) Secreted amyloid beta-protein similar to that in the senile plaques of Alzheimer's disease is increased in vivo by the presenilin 1 and 2 and APP mutations linked to familial Alzheimer's disease. Nat Med 2:864-870.

Stewart PA, Hayakawa K, Akers MA, Vinters HV (1992) A morphometric study of the blood-brain barrier in Alzheimer's disease. Lab Invest 67:734-742.

Szczepanik AM, Funes S, Petko W, Ringheim GE (2001) IL-4, IL-10 and IL-13 modulate A beta(1--42)-induced cytokine and chemokine production in primary murine microglia and a human monocyte cell line. J Neuroimmunol 113:49-62.

Thomas T, Sutton ET, Bryant MW, Rhodin JA (1997) In vivo vascular damage, leukocyte activation and inflammatory response induced by beta-amyloid. Journal of submicroscopic cytology and pathology 29:293-304.

Togo T, Akiyama H, Iseki E, Kondo H, Ikeda K, Kato M, Oda T, Tsuchiya K, Kosaka K (2002) Occurrence of T cells in the brain of Alzheimer's disease and other neurological diseases. J Neuroimmunol 124:83-92.

Town T, Laouar Y, Pittenger C, Mori T, Szekely CA, Tan J, Duman RS, Flavell RA (2008) Blocking TGF-beta-Smad2/3 innate immune signaling mitigates Alzheimer-like pathology. Nat Med 14:681-687.

Vinters HV, Wang ZZ, Secor DL (1996) Brain parenchymal and microvascular amyloid in Alzheimer's disease. Brain Pathol 6:179-195.

Wei R, Jonakait GM (1999) Neurotrophins and the anti-inflammatory agents interleukin-4 (IL-4), IL-10, IL-11 and transforming growth factor-beta1 (TGF-beta1) down-regulate T cell costimulatory molecules B7 and CD40 on cultured rat microglia. J Neuroimmunol 95:8-18.

Wisniewski HM, Kozlowski PB (1982) Evidence for blood-brain barrier changes in senile dementia of the Alzheimer type (SDAT). Ann N Y Acad Sci 396:119-129.

Yamamoto M, Kiyota T, Horiba M, Buescher JL, Walsh SM, Gendelman HE, Ikezu T (2007) Interferon-gamma and tumor necrosis factor-alpha regulate amyloid-beta plaque deposition and beta-secretase expression in Swedish mutant APP transgenic mice. Am J Pathol 170:680-692.

Zang YC, Samanta AK, Halder JB, Hong J, Tejada-Simon MV, Rivera VM, Zhang JZ (2000) Aberrant T cell migration toward RANTES and MIP-1 alpha in patients with multiple sclerosis. Overexpression of chemokine receptor CCR5. Brain 123 (Pt 9):1874-1882.

Zlokovic BV (2002) Vascular disorder in Alzheimer's disease: role in pathogenesis of dementia and therapeutic targets. Adv Drug Deliv Rev 54:1553-1559.

Zotova E, Holmes C, Johnston D, Neal JW, Nicoll JA, Boche D (2011) Microglial alterations in human Alzheimer's disease following Abeta42 immunization. Neuropathol Appl Neurobiol 37:513-524.

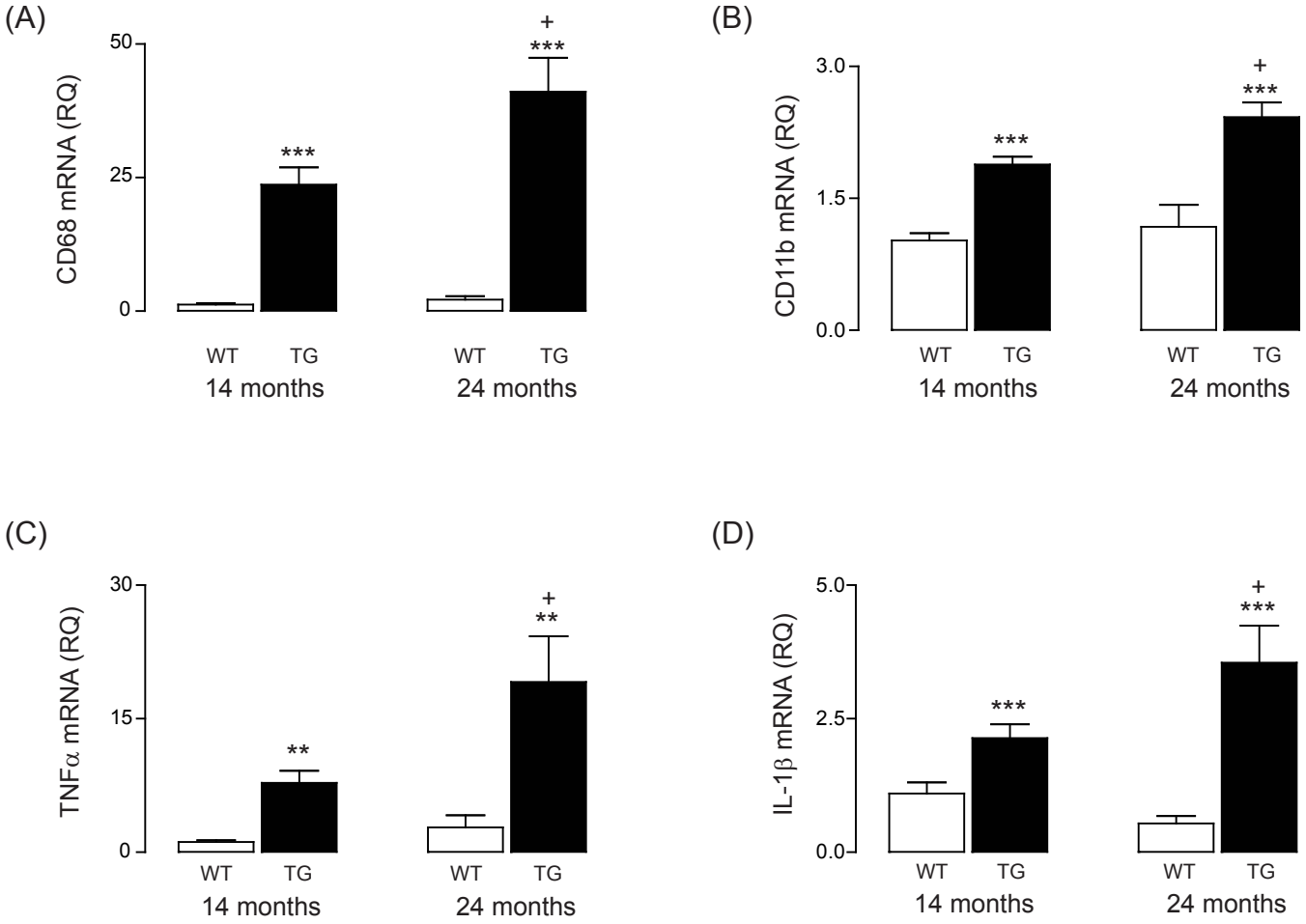
(A)
CD68 mRNA (RQ)
50
25
0
***
+
***
WT
TG
14 months
24 months
(B)
CD11b mRNA (RQ)
3.0
1.5
0.0
***
+
***
WT
TG
14 months
24 months
(C)
TNFα mRNA (RQ)
30
15
0
**
+
**
WT
TG
14 months
24 months
(D)
IL-1β mRNA (RQ)
5.0
2.5
0.0
***
+
***
WT
TG
14 months
24 months

Figure 1

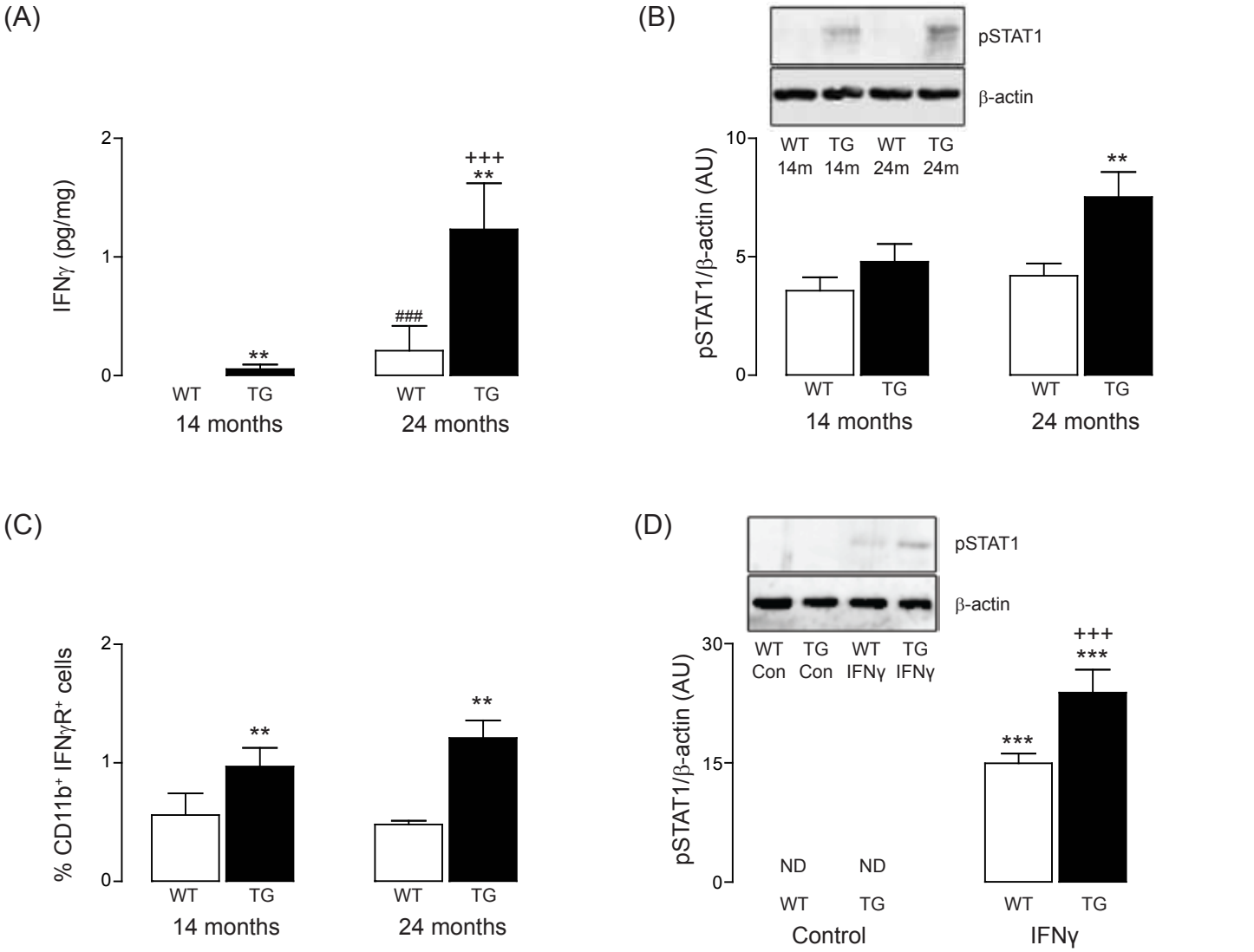
(A)
IFNγ (pg/mg)
2
1
0
**
###
+++
**
WT
TG
WT
TG
14 months
24 months
(B)
pSTAT1
β-actin
WT 14m
TG 14m
WT 24m
TG 24m
pSTAT1/β-actin (AU)
10
5
0
**
WT
TG
WT
TG
14 months
24 months
(C)
% CD11b+ IFNγR+ cells
2
1
0
**
**
WT
TG
WT
TG
14 months
24 months
(D)
pSTAT1
β-actin
WT Con
TG Con
WT IFNγ
TG IFNγ
pSTAT1/β-actin (AU)
30
15
0
***
+++
***
ND
ND
WT
TG
WT
TG
Control
IFNγ

Figure 2

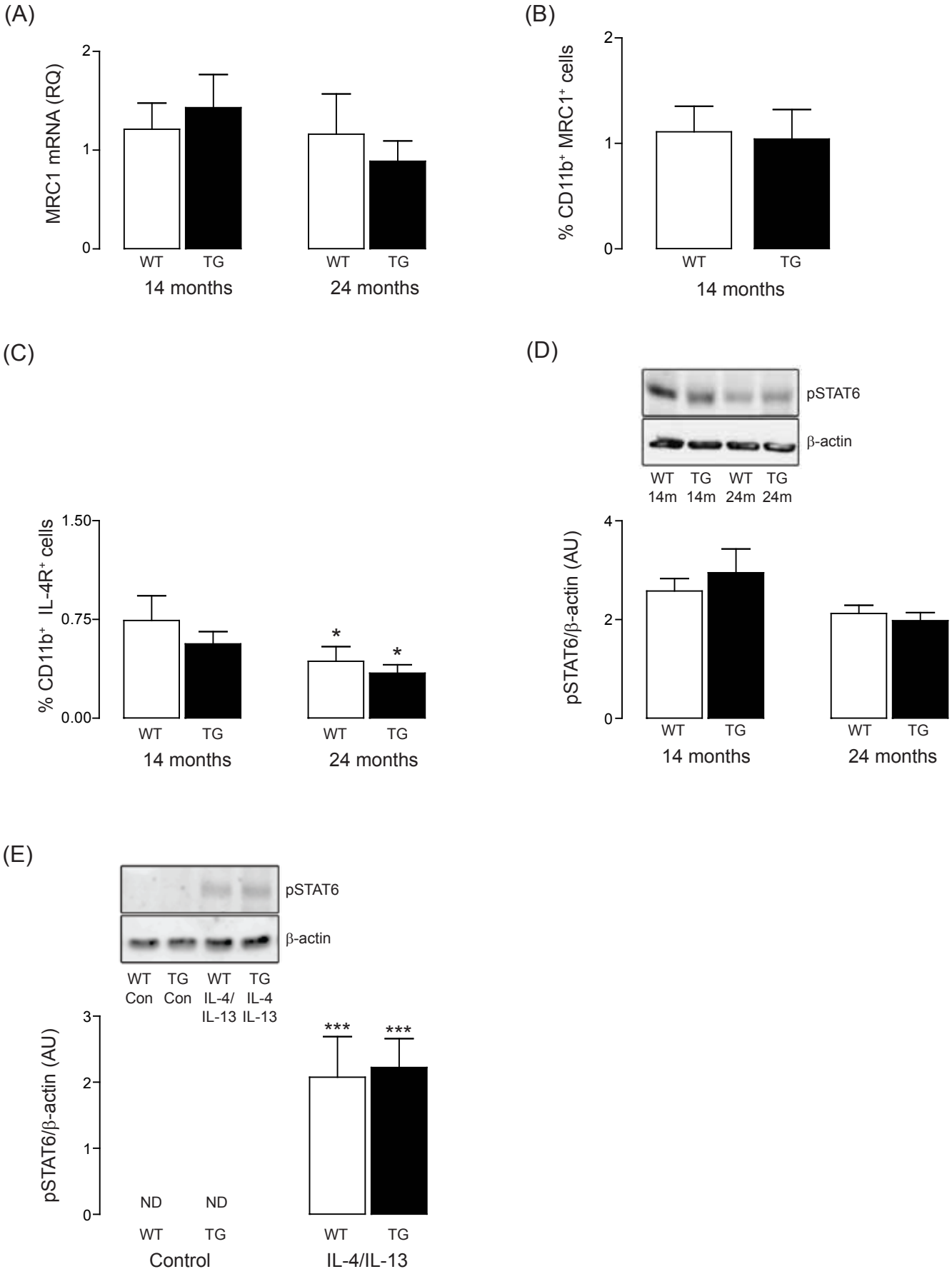
(A)
MRC1 mRNA (RQ)
2
1
0
WT
TG
WT
TG
14 months
24 months
(B)
% CD11b+ MRC1+ cells
2
1
0
WT
TG
14 months
(C)
% CD11b+ IL-4R+ cells
1.50
0.75
0.00
*
*
WT
TG
WT
TG
14 months
24 months
(D)
pSTAT6
β-actin
WT 14m
TG 14m
WT 24m
TG 24m
pSTAT6/β-actin (AU)
4
2
0
WT
TG
WT
TG
14 months
24 months
(E)
pSTAT6
β-actin
WT Con
TG Con
WT IL-4/ IL-13
TG IL-4 IL-13
pSTAT6/β-actin (AU)
3
2
1
0
***
***
ND
ND
WT
TG
WT
TG
Control
IL-4/IL-13

Figure 3

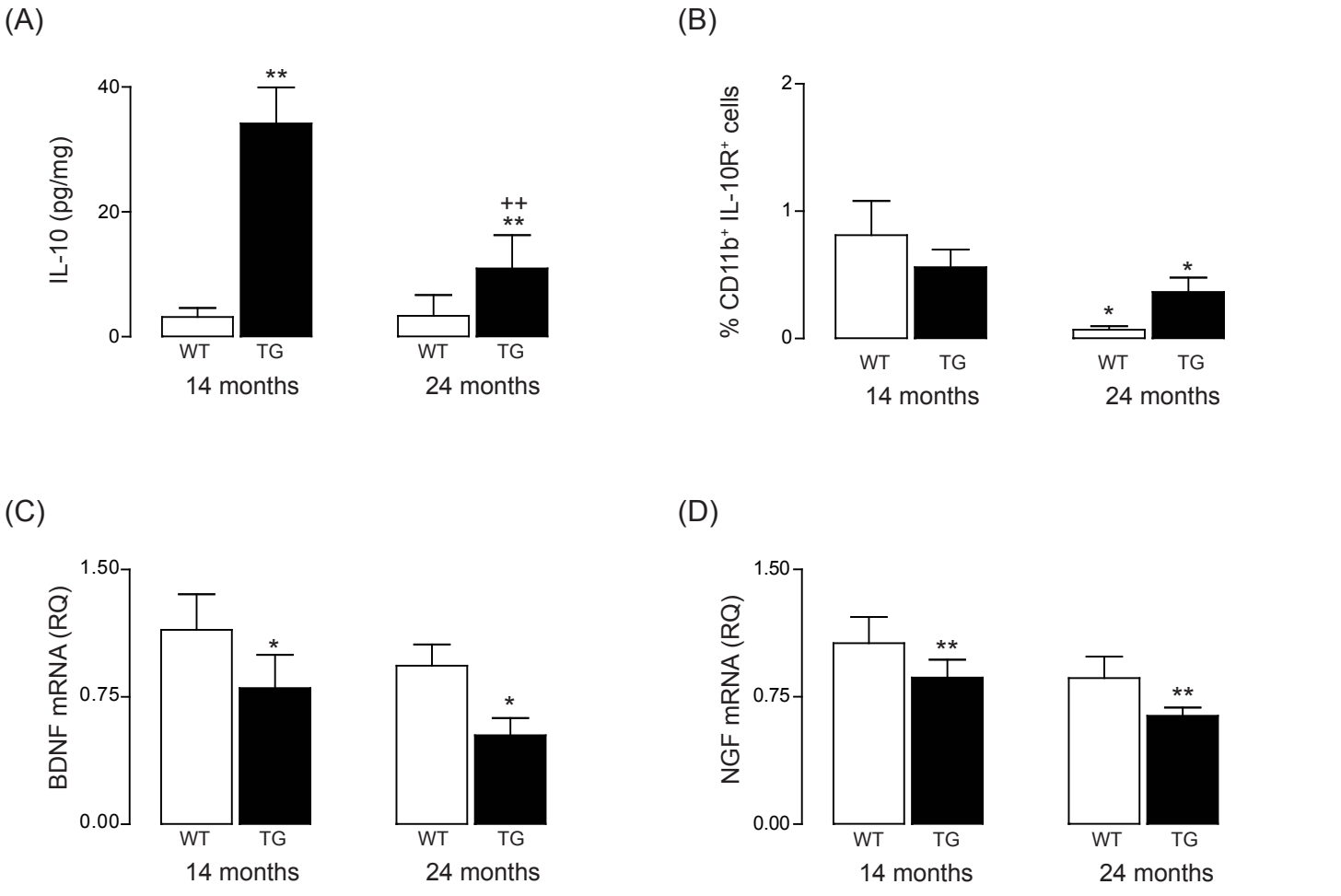

Figure 4

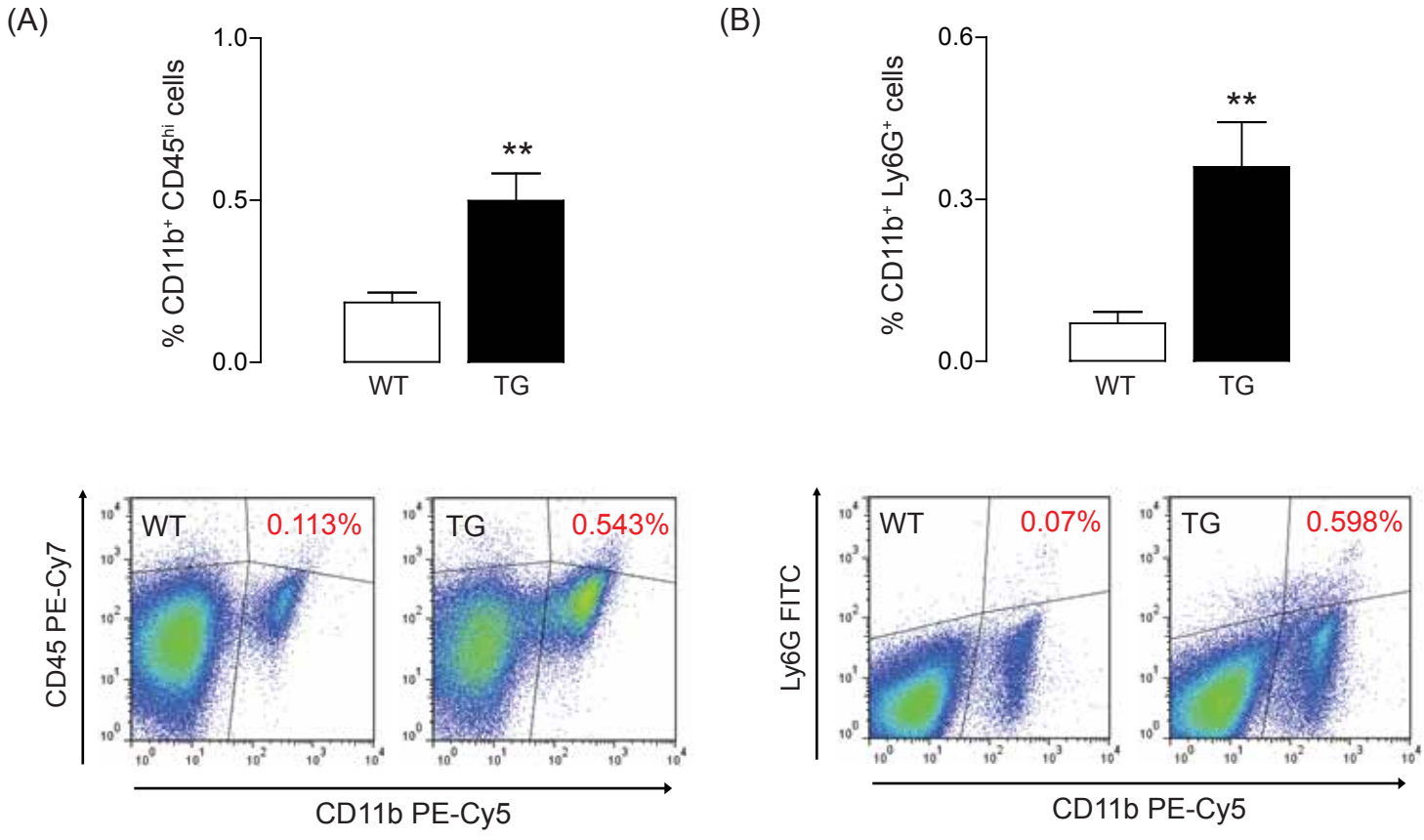

Figure 5

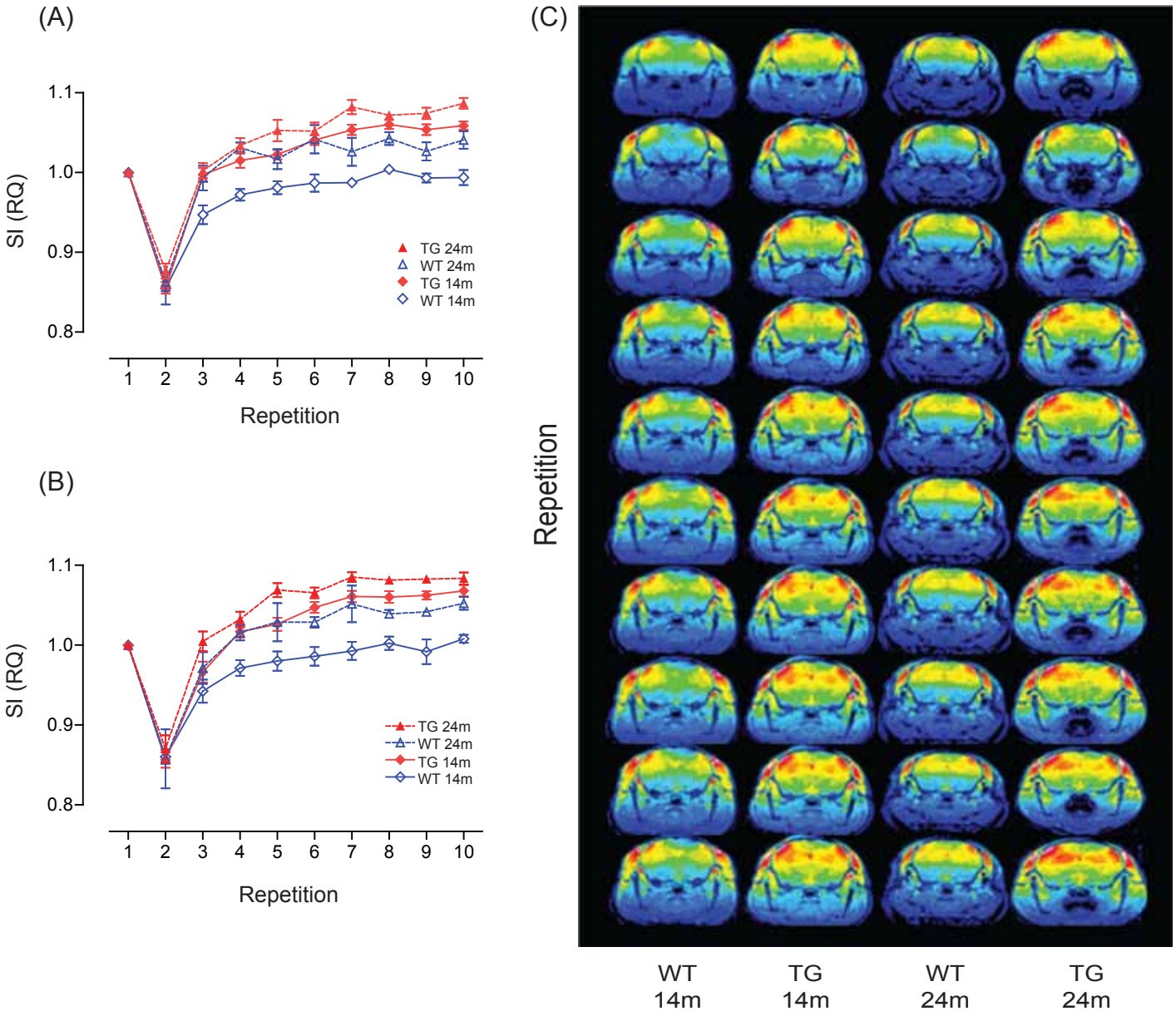
(A)
SI (RQ)
1.1
1.0
0.9
0.8
1 2 3 4 5 6 7 8 9 10
Repetition
TG 24m
WT 24m
TG 14m
WT 14m
(B)
SI (RQ)
1.1
1.0
0.9
0.8
1 2 3 4 5 6 7 8 9 10
Repetition
TG 24m
WT 24m
TG 14m
WT 14m
(C)
Repetition
WT 14m
TG 14m
WT 24m
TG 24m
(D)
WT
TG

Figure 6

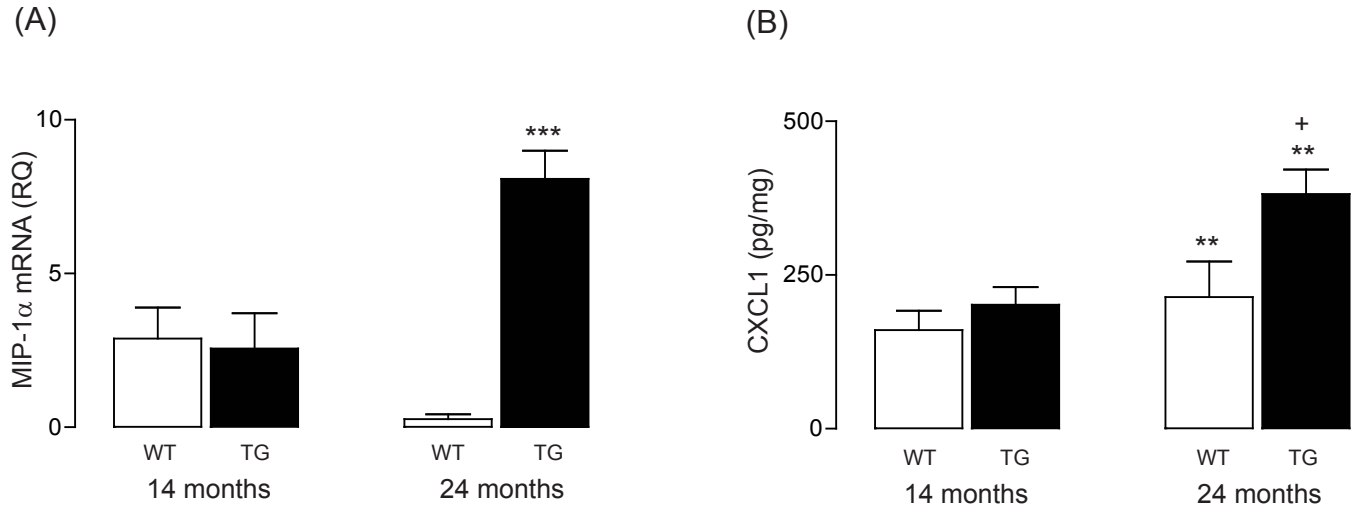

Figure 7

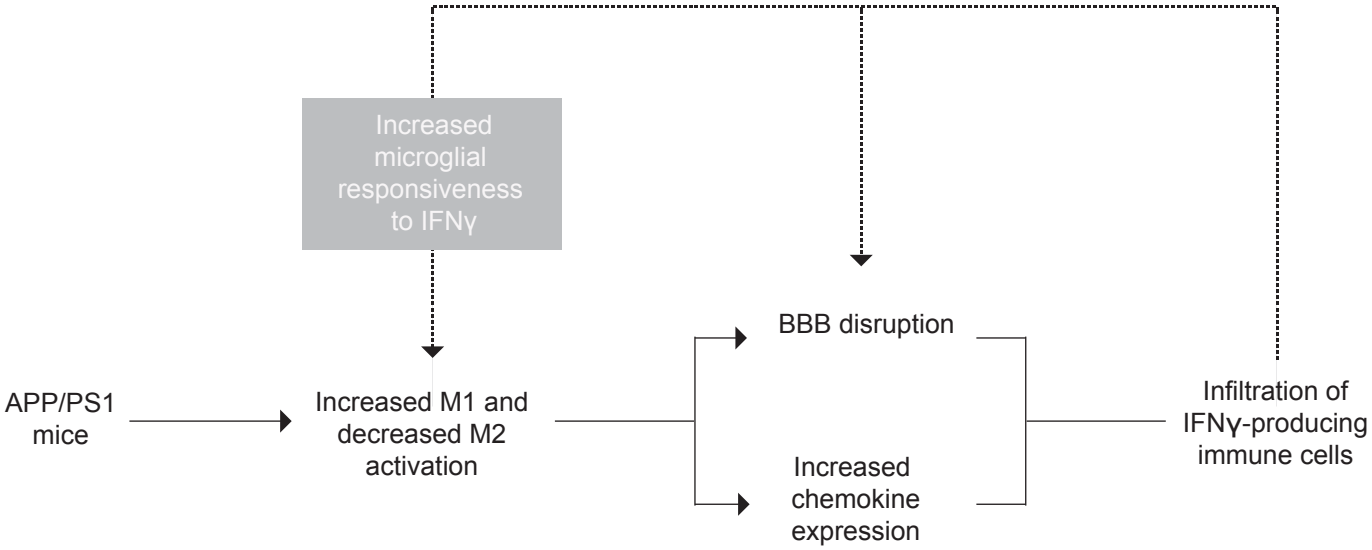

Figure 8

	WT 14 mo	**TG 14 mo**	**WT 24 mo**	**TG 24 mo**
Soluble $A\beta_{1\text{-}40}$	0.4241 ± 0.01	26.80 ± 3.4***	0.5150 ± 0.06	66.67 ± 11.2***,+++
Insoluble $A\beta_{1\text{-}40}$	2.674 ± 0.5	356.5 ± 92.2***	2.493 ± 0.8	737.4 ± 143.8***,+
Soluble $A\beta_{1\text{-}42}$	0.1236 ± 0.005	36.36 ± 5.3***	0.1661 ± 0.04	53.71 ± 2.1***,++
Insoluble $A\beta_{1\text{-}42}$	0.6123 ± 0.1	402.0 ± 70.4***	0.7328 ± 0.2	726.7 ± 133.1***,+

Table 1